



## Structure and spin in small iron clusters

P. Ballone, R.O. Jones

*Institut für Festkörperforschung, Forschungszentrum Jülich, D-52425 Jülich, Germany*

Received 29 November 1994

---

### Abstract

Density functional calculations have been performed for iron clusters with up to seven atoms. The electron–ion interaction is treated by a pseudopotential, and the large effect of core electrons on the spin configuration by modifying the exchange–correlation function. The scheme allows us to perform molecular dynamics (MD, Car–Parrinello) simulations and to explore the potential energy surface of the cluster without symmetry or other constraints. The most stable structures have magnetic moments  $\approx 3\mu_B$  per atom and are generally compact. We discuss the structural trends, particularly the similarities with the close-packed structures found in clusters where the atoms interact with a pairwise Lennard-Jones potential.

---

### 1. Introduction

Clusters  $X_n$ , comprising  $n$  atoms of element  $X$ , often have properties between those of bulk systems and the constituent atoms and have aroused much interest in recent years<sup>1</sup>. The relationship between the geometrical and spin structures is evident in clusters of the main group elements aluminium and gallium, where density functional (DF) calculations predict that the most stable isomers show a transition near  $n = 6$  from states with relative high spin degeneracy to states with the lowest possible spin [2]. It is understandable, however, that most work in this field has been devoted to studies of transition elements<sup>2</sup>, particularly those – such as iron – that are ferromagnetic in the bulk.

The variation of the properties of iron clusters with increasing number of atoms has been observed in a variety of contexts. Laser photoionization spectra of small iron clusters ( $Fe_2$ – $Fe_{25}$ ) show obvious changes in the ionization potential [4], there are marked changes in the reactivity with hydrogen and the binding energies with ammonia and water in clusters up to  $Fe_{23}$  [5], and collision-induced dissociation (CID) of  $Fe_n^+$ ,  $n = 2$ –19 show remarkable variations in the bond energies of both charged and neutral Fe clusters [6]. All these results can be viewed as evidence for changes in the geometrical structure as  $n$  increases. The CID work also provides evidence of at least one additional isomer in clusters with more than five atoms, with less stable isomers contributing 20%–35% of the ion beam in clusters larger than  $Fe_{12}$ .

The observation of Stern–Gerlach deflection of size-selected Fe clusters has provided a wealth of results on the spin structure of these systems, including detailed information on the size and temperature dependence of the magnetic moment and a compari-

---

<sup>1</sup> For a recent survey, see Ref. [1].

<sup>2</sup> For surveys of earlier work on transition metal clusters, see Ref. [3].

son with the other ferromagnetic elements Ni and Co [7]. At low temperature  $T$ , the magnetic moment per atom in the range  $25 \leq n \leq 700$  is *greater* than the bulk value, approaching the latter with slow oscillations as  $n$  increases. With increasing  $T$  the magnetic moments display a broad transition around a temperature in the general area of the bulk Curie point. Mössbauer spectroscopy of iron particles down to about 20 Å ( $n \approx 350$ ) show properties that are similar to those of bulk  $\alpha$ -Fe, although the anisotropy of the magnetic hyperfine field increased with decreasing particle size [8]. Clusters in the size range discussed here should have a large variety of both structural isomers and spin degeneracy and present ideal systems for studying the interplay of these two aspects.

A prerequisite for a detailed understanding of these problems is the ability to perform calculations – preferably without adjustable parameters – on clusters of a wide range of sizes, structures and spin degeneracies. This presents a computational task of formidable proportions. The number of electrons involved means that calculations using correlated wave functions (configuration interaction, CI) are very difficult to perform, although recent work [9] has shown that a satisfactory description of bonding in the  $\text{Fe}_2$  dimer can be obtained. Density functional calculations with a local spin density (LSD) approximation for the exchange–correlation energy [10] have been presented by Chen et al. [11] for iron clusters up to  $\text{Fe}_4$ . A comparison of different spin and geometrical structures indicated that states with ferromagnetic ordering and higher dimensionality (with longer bonds and more nearest-neighbour bonds) were favoured. Similar results were found in a study of  $\text{Fe}_n$  and singly charged ions up to  $n = 5$  [12]. While the bonds in  $\text{Fe}_2$ – $\text{Fe}_4$  were much shorter than the nearest-neighbour separation in bulk iron, bonds in some isomers of  $\text{Fe}_5$  had lengths near the bulk value. Calculations on larger clusters have been restricted to parameterized molecular dynamics work on transition metal clusters with six and seven atoms [13], and to a number of structures of  $\text{Fe}_{13}$  [14] and  $\text{Fe}_{15}$  [15]. Much remains to be done – in both theory and experiment – before we have a detailed understanding of the interplay between geometry and magnetism in these clusters.

We report here on density functional calculations

on iron clusters with up to seven atoms using a simulated annealing approach based on the work of Car and Parrinello [16]. This approach has been applied in our institute and elsewhere to clusters of main-group elements, examples being work on phosphorus and arsenic<sup>3</sup>. In these cases, the simulated annealing technique allowed us to find unexpected, stable structures. The present application to iron clusters has three main aims: (a) To show that reliable calculations for transition elements can be performed with a carefully constructed pseudopotential description of the electron–ion interaction; (2) to study the differences between pseudopotential and all-electron calculations in systems with large spin polarizations; and (3) to extend our present knowledge of bonding and structure in small iron clusters. Some of the structures found here are related to those found in clusters of atoms interacting via a Lennard-Jones potential [20]. The calculations are being extended to clusters with up to ten atoms, and the results will be reported when the work is complete.

## 2. Computational details

The method uses a basis set of plane waves and a pseudopotential description of the electron–ion interaction. Pseudopotentials constructed by Bachelet et al. [21] have been used in much of our earlier work and have proved to be satisfactory in many main group elements. In Fe, however, this form has a rapid spatial variation and would require an unacceptably large plane wave expansion. We have used instead a pseudopotential constructed along the lines prescribed by Troullier and Martins [22].

The reliability of pseudopotential calculations for magnetic properties has been questioned by Weinert et al. [23]. These authors performed calculations for the (001) surfaces of Rh and Fe using all-electron and pseudopotential methods and found that the magnetic moments are overestimated substantially by the latter. The origin of this discrepancy can be

<sup>3</sup> For  $\text{P}_2$ – $\text{P}_8$ ,  $\text{P}_9$ – $\text{P}_{11}$ , and  $\text{P}_n$  and  $\text{As}_n$  see Refs. [17–19], respectively.

traced to the differences in the spin polarization function

$$\zeta = \frac{|n_+ - n_-|}{n_+ + n_-}, \quad (1)$$

where  $n_+$  and  $n_-$  are the spin-up and spin-down components, respectively, of the total density  $n$ . Outside a very small central region, the numerator in Eq. (1) is determined primarily by the partially filled and easily polarizable valence states and is very similar in both cases. The denominator, however, is the total charge density and the differences can be substantial. The valence d states overlap significantly the highest-lying ‘core’ states (3p in the case of Fe), so that calculated spin polarizations are much higher in pseudopotential calculations than in those where all electrons are included.

A solution to the problem by including non-linear core corrections [24] would increase significantly the (already large) computational effort. An alternative approach is suggested by the observation that the error is important only at relatively short distances from the nuclei. It should be possible to modify the relationship between spin polarization  $\zeta$  and density  $n$  by assuming that

$$\zeta = \frac{|n_+ - n_-|}{g(n)}, \quad (2)$$

where

$$g(n) = n + \frac{n^2}{n_0 + n} \quad (3)$$

corrects for the overestimate of  $\zeta$  for valence densities larger than  $n_0$ . This last parameter allows us to optimize the agreement between pseudopotential and all-electron calculations. We have adopted the value 0.32 electron/au<sup>3</sup>, which leads to a change within a sphere of radius  $\approx 2$  au, around each Fe nucleus. We now discuss the effects on calculations for different states of the Fe atom.

The pseudopotential used in the present calculations reproduces accurately the 3d and 4s eigenvalues of all-electron calculations for the state of the Fe atom with  $S = 0$ . A comparison of all-electron and pseudopotential calculations for the  $S = 2$  and  $S = 4$  states illustrates the points we have made above. While the 4s eigenvalues are very similar in all-electron

and pseudopotential calculations, both the splitting of the 3d<sup>+</sup> and 3d<sup>-</sup> eigenvalues and the relative stabilities of the spin-polarized states are overestimated by approximately a factor of two. The energy difference between the  $S = 4$  and  $S = 0$  states, for example, is 0.267 au using the unmodified pseudopotential and 0.120 au in an all-electron calculation. Most of the discrepancies are removed by the simple modification (2). The eigenvalues agree to within 0.03 au in all cases, and the total energy difference between the above two states is 0.100 au.

We have used a simple cubic unit cell with lattice constant 20 au in all calculations. The plane wave expansion for the electron orbitals has an energy cutoff of 35 au (a total of 79 000 plane waves), and the electron density and the Kohn–Sham potential have been expanded with a cutoff of 112 au. The bonds in the structures shown in the figures represent nearest-neighbour separations of 4.6 au or less (the nearest-neighbour separation in bulk Fe at 20° is 4.69 au [25]), and the spheres showing the atoms have radii of 0.8 au. The numeration of the atoms has been chosen to facilitate structural comparisons. For the same reason we give the binding energies of clusters with  $n > 2$  as *cohesive* energies  $E_{\text{coh}}$ , the binding energies *per atom*.

### 3. Results

#### 3.1. The Fe<sub>2</sub> dimer

Although the iron dimer has been used on many occasions as a test case for computational schemes, experimental information on Fe<sub>2</sub> is not extensive. The bond lengths in argon and neon matrices are 3.53 au [26] and 3.82 au [27] respectively, and the most recent estimate of the bond energy in the gas phase is  $1.14 \pm 0.10$  eV [6]. Photoelectron detachment from Fe<sub>2</sub><sup>-</sup> [28] provides information about the electron affinity of Fe<sub>2</sub> and the vibrational frequencies of Fe<sub>2</sub> and Fe<sub>2</sub><sup>-</sup>. Calculations using correlated wave functions are very difficult to perform for such systems, but a recent calculation (configuration interaction (CI) with quadruple excitations) [9] indicated a <sup>7</sup>Δ<sub>u</sub> ground state (bond length  $r_e = 3.89$  au, bond strength  $D_e = 1.57$  eV).

The Fe<sub>2</sub> molecule has been the subject of several

density functional calculations, most of which use a local spin density approximation for the exchange–correlation energy. The first [29] suggested a  ${}^7\Delta_u$  ground state with  $r_e = 3.96$  au and  $D_e = 3.45$  eV. However, the subtle balance between the tendency to occupy the maximum number of bonding orbitals (which usually leads to low-spin states) and Hund’s multiplicity rule (which seeks to maximize the spin multiplicity) means that other states have similar energies. LSD calculations by Dhar and Kestner [30] also predicted a  ${}^7\Delta_u$  ground state ( $r_e = 3.70$  au,  $D_e = 2.89$  eV). The importance of the effects of spin is shown by a comparison of the results of Chen et al. [11] for the spin-polarized (‘ferromagnetic’,  $S = 3$ ) state (3.74 au, 4.05 eV) and the spinless (‘paramagnetic’,  $S = 0$ ) state (3.46 au, 1.73 eV). Similar bond lengths were found by Castro and Salahub [12] (3.70 and 3.40 au, respectively), whose calculations with a non-local approximation for the exchange–correlation energy gave slightly longer bonds (3.79 au and 3.46 au, respectively). With respect to two non-spherical ( ${}^5D$ ) atoms, the non-local approximation gives a  $D_e$  value of 2.08 eV.

If we use the conventional definition of the spin-polarization  $\zeta$ , we obtain for the  $S = 0$  state  $r_e = 3.545$  au,  $D_e = 1.64$  eV, and for  $S = 3$  the values 3.85 au, 4.02 eV. Using the definition (2), we find 3.80 au and 3.81 eV for  $S = 3$ . Of the other states calculated, the most stable with  $S = 4$  has (3.89 au, 3.56 eV). The most stable with  $S = 2$  is much higher in energy ( $D_e = 1.90$  eV). The main effect of the modified form (2) in  $Fe_2$  is to reduce the binding energy of the ground state by 0.2 eV.

### 3.2. $Fe_3$

For the iron trimer, earlier calculations give a  $C_{3v}$  (equilateral triangle) ground state with  $S = 4$ . Chen et al. [11] find  $r_e = 3.86$  au,  $E_{coh} = 2.60$  eV, Castro and Salahub [12]  $r_e = 3.97$  au, and a value of  $E_{coh} = 1.41$  eV for a non-local functional relative to a non-spherical atom.

In the present calculations, three  $C_{3v}$  isomers with different spins are the most stable. With the conventional definition of  $\zeta$ , we find a state with  $S = 4$ ,  $r_e = 4.13$  au, and  $E_{coh} = 2.47$  eV. With the modified form (2), the most stable state (Fig. 1a) has  $S = 4$ ,  $r_e = 4.04$  au, and  $E_{coh} = 3.04$  eV.  $C_{3v}$  structures

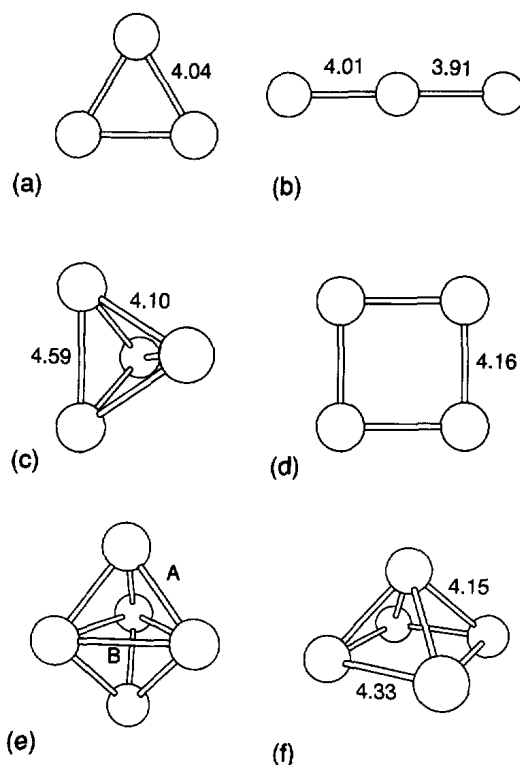


Fig. 1. Structures of  $Fe_3$  ((a) and (b)),  $Fe_4$  ((c) and (d)),  $Fe_5$  (e), trigonal bipyramid ( $D_{3h}$ ). A and B denote lengths of diagonal and base, respectively. (f)  $Fe_5$ , pyramid.

with higher ( $S = 5$ ) and lower ( $S = 3$ ) spins lie higher in energy, with  $E_{coh}$  and  $r_e$  values of (2.91 eV, 4.08 au) and (2.42 eV, 3.98 au), respectively. There is a spin-free ( $S = 0$ ) state with  $C_{3v}$  symmetry, with a shorter bond (3.84 au) and a much higher energy ( $D_e = 4.44$  eV). We were surprised to find a linear, asymmetric form ( $C_{\infty v}$ ) with  $S = 4$  and  $E_{coh} = 2.35$  eV (Fig. 1b).

### 3.3. $Fe_4$

The previously published calculations predict that the most stable isomer of  $Fe_4$  is tetrahedral ( $T_d$ ) with  $S = 6$ . Chen et al. [11] found a bond length of 4.25 au, with  $E_{coh} = 3.07$  eV, while Castro and Salahub [12] found  $r_e = 4.20$  au and a value of  $E_{coh}$  – relative to non-spherical atoms and with a non-local functional – of 2.49 eV.

In the present calculations, the tetrahedral structure proved to be unstable to annealing at temperatures  $\approx 500$  K. The tetrahedron opened up into the

butterfly ( $C_{2v}$ ) structure shown in Fig. 1c, with  $S = 6$  and  $E_{\text{coh}} = 3.55$  eV. The ‘wings’ of the butterfly open up slightly if  $S = 7$ , leading to a structure lying 0.10 eV/atom higher. A more compact structure with  $S = 5$  has an energy a further 0.13 eV/atom higher. A square structure with  $r_e = 4.16$  au (Fig. 1d) lies 0.74 eV/atom above the most stable ( $C_{2v}$ ) structure.

### 3.4. $Fe_5$

Calculations of the iron pentamer have been performed by Castro and Salahub [12]. The most stable isomer that they found was a distortion of a  $D_{3h}$  trigonal bipyramid with  $S = 8$  and  $E_{\text{coh}} = 3.59$  eV/atom. A more compact distorted  $D_{3h}$  structure with  $S = 7$  is almost degenerate, followed by a square pyramid ( $C_{4v}$ ,  $S = 9$ , 0.06 eV/atom) and a compressed pentagon (0.25 eV/atom) higher in energy.

The present calculations lead to a similar picture, with differences in detail. We have found four minima with the trigonal bipyramid structure shown in Fig. 1e, with diagonals ( $A$ ) and bases ( $B$ ) of differing lengths. The most stable of these ( $E_{\text{coh}} = 3.90$  eV/atom,  $A = 4.16$  au,  $B = 4.37$  au) has  $S = 7$ . We found two different minima with both this symmetry and  $S = 8$  (3.88 eV/atom, 4.17, 4.40; 3.39 eV/atom, 4.26, 4.56) and one with  $S = 9$  (3.57 eV, 4.18, 4.42). The cohesive energies of the pyramid ( $S = 8$ , Fig. 1f) and the regular pentagon ( $S = 8$ , Fig. 2a) are 3.64 and 3.24 eV/atom, respectively.

### 3.5. $Fe_6$

Apart from the work of Sawada and Sugano [13], which uses a parameterized form of the interatomic interactions, we know of no calculations of the hexamer and heptamer that incorporate geometry optimization. The most stable structure that we found (with  $S = 10$ ) is shown in Fig. 2b and was the first we encountered without axial symmetry. It may be viewed as a capping of the trigonal bipyramid form (Fig. 1e) of  $Fe_5$ , and has  $E_{\text{coh}} = 4.01$  eV/atom and the following internuclear separations (in au): 4.08 ( $r_{46}, r_{36}$ ), 4.15 ( $r_{14}, r_{15}, r_{24}, r_{25}$ ), 4.29 ( $r_{34}$ ), 4.34 ( $r_{35}$ ), 4.42 ( $r_{12}, r_{13}, r_{23}, r_{16}$ ). Only 0.02 eV/atom higher in energy (also with  $S = 10$ ) was the compressed octahedron ( $D_{4h}$ ) shown in Fig. 2c. Opti-

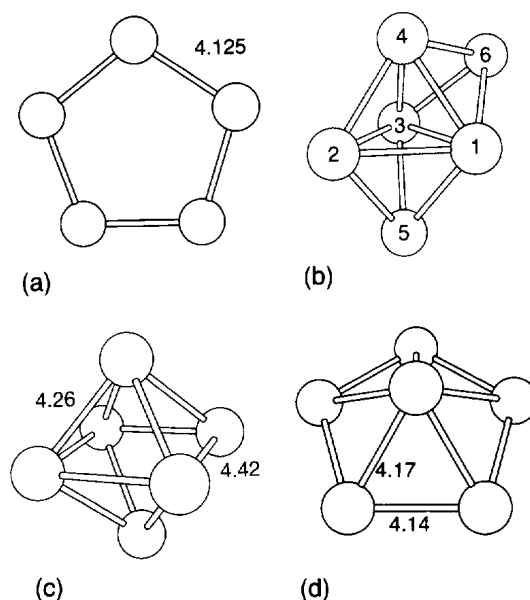


Fig. 2. Structures of (a)  $Fe_5$ , regular pentagon, (b)  $Fe_6$  ( $C_1$ ), (c)  $Fe_6$  compressed octahedron ( $D_{4h}$ ), (d)  $Fe_6$ , pentagonal pyramid.

mization of this geometry with  $S = 9$  leads to a cohesive energy of 3.88 eV/atom, with  $S = 11$  of 3.06 eV/atom. The capped pentagon (Fig. 2a) was also stable, with  $E_{\text{coh}} = 3.90$  eV/atom.

### 3.6. $Fe_7$

We found several structures for the heptamer, and the most stable are shown in Fig. 3. The most stable is a pentagonal bipyramid ( $D_{5h}$ , Fig. 3a), which has  $S = 11$  and  $E_{\text{coh}} = 4.37$  eV and is the most compact capping of the isomer of  $Fe_6$  with the lowest energy. The distance  $r_{13}$  is 4.48 au. Structures in Fig. 3b ( $C_s$ ) and in Figs. 3c and 3d (a distortion of  $C_2$  as discussed below) have  $S = 11$  and almost equal energies (cohesive energies of 4.26 and 4.23 eV/atom, respectively). They are different cappings of the same hexamer structure (Fig. 2b) and have bond lengths remarkably closely related to those in this cluster. The bonds in the  $C_s$  structure, for example, are unchanged and the bonds between atom 7 and its neighbours are the same as those connecting atom 6 to its neighbours. The same is true in the other capped structure, shown from two perspectives in Figs. 3c and 3d. There appears to be a small distortion of the twofold rotational symmetry, with  $r_{24}$

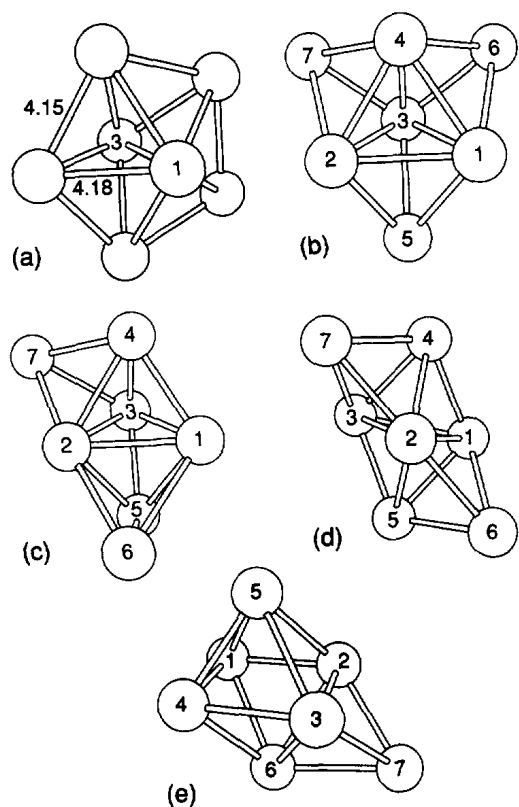


Fig. 3. Structures of  $\text{Fe}_7$ . (a) Pentagonal bipyramid ( $C_{5h}$ ); (b) 'incomplete stellated tetrahedron' ( $C_s$ ); ((c) and (d)) 'skewed' structure ( $\sim C_2$ ); (e) capped octahedron ( $C_s$ ). The structure designations quoted are those of Ref. [20].

being  $\approx 1\%$  shorter than  $r_{34}$  in the other clusters. The bonds lengths are otherwise remarkably transferable. The remaining structure (Fig. 3e,  $C_s$  symmetry) may be viewed as a capping of the compressed octahedron (Fig. 2c). It lies 0.14 eV/atom above the other  $C_s$  structure and has bond lengths (au) 4.16 ( $r_{56}, r_{67}$ ), 4.20 ( $r_{13}$ ), 4.28 ( $r_{24}, r_{26}, r_{46}$ ), 4.30 ( $r_{35}, r_{37}$ ), 4.34 ( $r_{23}, r_{34}$ ), 4.41 ( $r_{24}$ ), 4.45 ( $r_{25}, r_{47}$ ), 4.48 ( $r_{12}, r_{14}$ ). In this case the additional atom has a larger influence on the bond lengths in the parent  $\text{Fe}_6$  structure.

#### 4. Discussion

The present Letter has described calculations of the energy surfaces and the geometries of isomers of iron clusters with up to seven atoms, with interesting results. Perhaps the most important is our demonstra-

tion that molecular dynamics (simulated annealing, SA) calculations can be performed for transition element clusters if one uses a carefully constructed pseudopotential. The experience with the structures of clusters of main-group elements, i.e., that SA can lead to stable structures that are unknown and unexpected, has been repeated here. Although no method can guarantee to find either the global minimum of a complicated energy surface or the local minima corresponding to all stable isomers, our experience indicates that annealing methods improve greatly the chances of both.

The results for the clusters up to  $n = 5$  are in satisfactory agreement with previous work, although the calculations for the tetramer indicate that the tetrahedral structures found previously are less stable than the 'butterfly' or 'roof' isomer ( $C_{2v}$ ). Compact clusters are generally more stable than open structures, an obvious example being the triangular structure in  $\text{Fe}_3$ , which is more stable than the linear form. This effect is also evident in  $\text{Fe}_7$ , where the structure with approximately  $C_2$  symmetry (referred to in other work [18] as 'skewed') is less stable than the more compact conformers.

It is not surprising that spin plays a crucial role in determining the most stable structures. Calculations performed *without* spin (LDA calculations) lead invariably to shorter bond lengths than those found in LSD calculations. We have given some examples above. The large spin energies that result from unpaired spins in transition elements (clusters and extended systems) often compensate for the reduction in the occupancy of bonding orbitals that this requires. The above results show that the magnetic moments in the clusters are approximately  $3 \mu_B$  per atom.

One of the most interesting results of the present work is, however, the striking similarity between the isomeric forms and those found in clusters where the interaction is modelled either by a pairwise Lennard-Jones potential [20] or by a form adjusted to have general validity for transition element clusters [13]. Both the LJ potential and the present results lead to qualitatively new geometries at the same cluster sizes: with  $n = 2, 3, 4$  we go from one- to three-dimensional geometries, with  $n = 5$  there is the first energy minimum with next nearest neighbours, and for  $n = 6$  the first without axial symmetry. Al-

though the energy ordering of the isomers is not always the same, the remarkable similarities suggest that the angular dependence of the forces in Fe clusters is weaker than in clusters of the elements with ‘covalent’ bonds (group III (Al, ...), IV (Si, ...), V (P, ...), and VI (S, ...)), which show distinctly different patterns.

Work on larger clusters up to Fe<sub>10</sub> is in progress. We shall present the results elsewhere, where we shall also provide more details about the trends found in the present study. It should be noted that the present calculations and the extension to ten-atom clusters require a very large investment in computing time and resources. With current computing technology, such a project is near the limit of the applicability to transition element clusters of SA methods that use a plane wave basis and a pseudopotential representation of the electron–ion interaction.

### Acknowledgement

We thank W.A. de Heer for discussions and the German Supercomputer Center (HLRZ) for a grant of CPU time on the Cray YMP8/864 in the Forschungszentrum Jülich.

### References

- [1] H. Haberland, ed., *Clusters of atoms and molecules* (Springer, Berlin, 1994).
- [2] R.O. Jones, *J. Chem. Phys.* 99 (1993) 1194.
- [3] M.D. Morse, *Chem. Rev.* 86 (1986) 1049; D.R. Salahub, *Advan. Chem. Phys.* 69 (1987) 477.
- [4] E.A. Rohlfing, D.M. Cox, A. Kaldor and K.H. Johnson, *J. Chem. Phys.* 81 (1984) 3846.
- [5] E.K. Parks, B.H. Weiller, P.S. Bechthold, W.F. Hoffmann, G.C. Nieman, L.G. Pobo and S.J. Riley, *J. Chem. Phys.* 88 (1988) 1622.
- [6] L. Lian, C.-X. Su and P.B. Armentrout, *J. Chem. Phys.* 97 (1992) 4072.
- [7] I.M.L. Billas, A. Châtelain and W.A. de Heer, *Science* 265 (1994) 1682.
- [8] F. Bødker, S. Mørup and S. Linderoth, *Phys. Rev. Letters* 72 (1994) 282.
- [9] T. Noro, C. Ballard, M.H. Palmer and H. Tatewaki, *J. Chem. Phys.* 100 (1994) 452.
- [10] For a review, see R.O. Jones and O. Gunnarsson, *Rev. Mod. Phys.* 61 (1989) 689.
- [11] J.L. Chen, C.S. Wang, K.A. Jackson and M.R. Pedersen, *Phys. Rev. B* 44 (1991) 6558.
- [12] M. Castro and D.R. Salahub, *Phys. Rev. B* 49 (1994) 11842.
- [13] S. Sawada and S. Sugano, *Z. Physik D* 14 (1989) 247.
- [14] B.I. Dunlap, *Phys. Rev. A* 41 (1990) 5691.
- [15] A. Ayuela, U. Lammers and G. Borstel, *Comput. Mat. Sci.* 2 (1994) 589.
- [16] R. Car and M. Parrinello, *Phys. Rev. Letters* 55 (1985) 2471.
- [17] R.O. Jones and D. Hohl, *J. Chem. Phys.* 92 (1990) 6710.
- [18] R.O. Jones and G. Seifert, *J. Chem. Phys.* 96 (1992) 7564.
- [19] P. Ballone and R.O. Jones, *J. Chem. Phys.* 100 (1994) 4941.
- [20] M.R. Hoare and P. Pal, *Advan. Phys.* 20 (1971) 161; *J. Cryst. Growth* 17 (1972) 77.
- [21] G.B. Bachelet, D.R. Hamann and M. Schlüter, *Phys. Rev. B* 26 (1982) 4199.
- [22] N. Troullier and J.L. Martins, *Phys. Rev. B* 43 (1991) 1993.
- [23] M. Weinert, S. Blügel and P.D. Johnson, *Phys. Rev. Letters* 71 (1993) 4097.
- [24] S.G. Louie, S. Froyen and M.L. Cohen, *Phys. Rev. B* 26 (1982) 1738.
- [25] J. Donohue, *The structures of the elements* (Wiley, New York, 1974) p. 205.
- [26] P.A. Montano and G.K. Shenoy, *Solid State Commun.* 35 (1980) 53.
- [27] H. Purdum, P.A. Montano, G.K. Shenoy and T. Morrison, *Phys. Rev. B* 25 (1982) 4412.
- [28] D.G. Leopold and W.C. Lineberger, *J. Chem. Phys.* 85 (1986) 51.
- [29] J. Harris and R.O. Jones, *J. Chem. Phys.* 70 (1979) 830.
- [30] S. Dhar and N.R. Kestner, *Phys. Rev. A* 38 (1988) 1111.